

The precision of slow-roll predictions for the CMBR anisotropies

Jérôme Martin

DARC, Observatoire de Paris,
UPR 176 CNRS, 92195 Meudon Cedex, France.
e-mail: martin@edelweiss.obspm.fr

Dominik J. Schwarz

Institut für Theoretische Physik,
Wiedner Hauptstraße 8 – 10, 1040 Wien, Austria.
e-mail: dschwarz@hep.itp.tuwien.ac.at
(November 5, 1999)

Inflationary predictions for the anisotropy of the cosmic microwave background radiation (CMBR) are often based on the slow-roll approximation. We study the precision with which the multipole moments of the temperature two-point correlation function can be predicted by means of the slow-roll approximation. We ask whether this precision is good enough for the forthcoming high precision observations (error $\leq 1\%$) by means of the MAP and PLANCK satellites. The error in the multipole moments due to the slow-roll approximation is demonstrated to be bigger than the error in the power spectrum. For power-law inflation with $n_S = 0.9$ the error from the leading order slow-roll approximation is $\approx 5\%$ for the amplitudes and $\approx 20\%$ for the quadrupoles. For the next-to-leading order the errors are within a few percent. The errors increase with $|n_S - 1|$. To obtain a precision of 1% it is mandatory to use the next-to-leading order. For a general model of inflation the next-to-leading order does not guarantee 1% precision. In the case of power-law inflation this precision is obtained for the spectral indices if $|n_S - 1| > 0.02$ and for the quadrupoles if $|n_S - 1| > 0.15$ only. The slow-roll approximation cannot be improved beyond the next-to-leading order in the slow-roll parameters.

PACS numbers: 98.80.Cq, 98.70.Vc

I. INTRODUCTION

During the next years, high precision measurements of the Cosmic Microwave Background Radiation (CMBR) anisotropies will be performed by the MAP and Planck satellites [1]. Observations from balloon borne experiments, such as Boomerang [2], will also supply us with high quality measurements over a large range of multipoles soon. Inflation [3] provides a mechanism to produce the primordial fluctuations of space-time and matter [4–7], which lead to the CMBR anisotropies and to the large scale structure. This mechanism rests on the principles of General Relativity and Quantum Field Theory. It thus can be expected to get a hand on the physics of the very early Universe with help of the upcoming high precision measurements.

The CMBR anisotropies are most conveniently expressed by the multipole moments C_l . The computation of the multipole moments requires the knowledge of the primordial spectrum and the transfer functions. The latter depend on the cosmological parameters $H_0, \Omega_M, \Omega_\Lambda, \dots$. The transfer function characterizes the evolution of cosmological perturbations during the radiation and matter epochs. The primordial spectrum is predicted by inflation and depends on the evolution of the long wavelength perturbations during inflation and reheating. It can be predicted from a given model of

inflation.

In this article, we will restrict our considerations to slow-roll inflation with one scalar field. This represents only a first step towards a more general study. Our aim is to address the following problems: What is the precision of the predicted multipole moments from the slow-roll approximation? Is this precision sufficient to reach the level of accuracy expected from the planned observations? Can the slow-roll approximation be improved to arbitrary precision?

So far, the precision of the predicted power spectrum has been examined by Grivell and Liddle [8]. However, the power spectrum is not directly observable whereas the C_l 's are. We show that the error from the slow-roll approximation is important in the multipole moments. It is bigger than the error in the power spectrum. It turns out that the next-to-leading order slow-roll approximation [9] is compulsory, but it may not be sufficient to reach an accuracy of a few % or less.

Wang, Mukhanov and Steinhardt [10] have shown that predictions based on the time delay argument [6] or on the horizon crossing/Bessel function approach (i.e. the slow-roll approximation) [9,11] are not reliable for general models of inflation. There have been various attempts to improve the slow-roll approximation to higher orders, see e.g. [9,12,13,11]. The conclusion of Wang et al. [10] has been contested by Copeland et al. [14]: “We . . . conclude

that any theoretical errors from the use of the slow-roll equations are likely to be subdominant". We show in this work that this claim is not correct unless the slow-roll parameters are extremely small. Typically, we find that the slow-roll parameters must be less than 0.01 in order for the next-to-leading order to reach the level of precision of MAP or PLANCK. This means that there exists space for models where the slow-roll error is dominant and the slow-roll approximation still valid. We find in agreement with the analysis in [10] that a slow-roll approximation that goes beyond the next-to-leading order cannot exist. All higher order corrections are thus meaningless. In the derivation of this result we close a gap in the proof of the next-to-leading order equations. For some reason this gap was not noted before in the literature. For this purpose we use and generalize a new family of exact solutions, which was recently found by Starobinsky [15].

The scope of this paper is to quantify the error from the slow-roll approximation. For this purpose we compute the scalar and tensor quadrupole moments and their ratio $R \equiv C_2^T/C_2^S$ for power-law inflation, for which the exact result is known. Then, we calculate the same quantities for the same model but in the context of the slow-roll approximation. The comparison of the two results provides an estimate of the error made by using the slow-roll approximation. We do not convolute this error with the uncertainties in the transfer functions. We therefore concentrate our attention to the quadrupole moments, where the influence of the transfer function is expected to be minimal. For the sake of clarity and simplicity we make use of the transfer functions in the long wavelength limit. We expect that for low multipoles the order of magnitude of the error in the inflationary prediction is the same.

This article is organized as follows: in the next section, the theory of cosmological perturbations and the calculations of the CMBR anisotropies are reviewed. Then, the low l multipole moments are computed exactly for power-law inflation (Sec. III) and approximatively for slow-roll inflation (Sec. IV). Comparison of the two results allows us to test the precision of the CMBR multipoles obtained from the slow-roll approximation in the last section. We set $c = \hbar = 1$ throughout the paper.

II. FROM QUANTUM FLUCTUATIONS TO CMBR ANISOTROPIES

The line element for the spatially flat Friedmann-Lemaître-Robertson-Walker (FLRW) background plus perturbations can be written as [7]:

$$ds^2 = a^2(\eta) \{ -(1 - 2\phi)d\eta^2 + 2(\partial_i B)dx^i d\eta + [(1 - 2\psi)\delta_{ij} + 2\partial_i \partial_j E + h_{ij}]dx^i dx^j \}. \quad (1)$$

In this equation, the functions ϕ , B , ψ and E represent the scalar sector whereas the tensor h_{ij} , satisfy-

ing $h_i^i = h_{ij}^j = 0$, represents the gravitational waves. There are no vector perturbations because a single scalar field cannot seed rotational perturbations. The conformal time η is related to the cosmic time t by $dt = a(\eta)d\eta$. It is convenient to introduce the background quantity $\gamma(\eta)$ defined by $\gamma \equiv -\dot{H}/H^2$, where a dot means differentiation with respect to cosmic time and H is the Hubble rate, $H \equiv \dot{a}/a$. Using conformal time we may write $\gamma = 1 - \mathcal{H}'/\mathcal{H}^2$, where $\mathcal{H} \equiv a'/a$, and a prime denotes differentiation with respect to the conformal time.

We assume that inflation is driven by a single scalar field. For the perturbations we introduce gauge-invariant variables [16,7], which reduce the equations of motion, in the small scale limit, to equations of harmonic oscillators [17–20,7]. In the tensor sector (which is gauge invariant) we define the quantity μ_T for each mode k according to $h_{ij} = (\mu_T/a)Q_{ij}(k)$, where $Q_{ij}(k)$ are the (transverse and traceless) eigentensors of the Laplace operator on the spacelike sections and k^2 is the corresponding eigenvalue. Gravitational waves do not couple to scalar fields. Thus the equation of motion is given by [17]:

$$\mu_T'' + \left[k^2 - \frac{a''}{a} \right] \mu_T = 0. \quad (2)$$

The scalar sector is gauge dependent and the scalar perturbations of the metric are coupled to the perturbations of the stress tensor describing the matter. Fluctuations in the stress tensor involve perturbations in the energy density, $\delta\rho$, and in the four velocity, $\delta u^\mu = (-\phi/a, v^i/a)$. We describe perturbations in the density contrast by the gauge invariant quantity $\delta \equiv \delta\rho/\rho + (\rho'/\rho)(B - E')$. Perturbations in the velocity can be written as $v_i \equiv \partial_i w + w_i$. Since we are interested in the scalar sector, only the first term has to be taken into account. We choose to work with the gauge invariant quantity $v \equiv w + E'$. Scalar perturbations of the geometry can be characterized by the two gauge invariant Bardeen potentials $\Phi Q \equiv \phi + (1/a)[(B - E')a]'$ and $\Psi Q \equiv \psi - \mathcal{H}(B - E')$ [16], where $Q(k)$ is a scalar harmonic. During inflation, the Universe is dominated by the scalar field $\varphi = \varphi_0(\eta) + \varphi_1(\eta)Q$. Fluctuations in the scalar field are characterized by the gauge invariant quantity $\delta\varphi \equiv \varphi_1 + \varphi_0'(B - E')$. In this simple case, the time evolution of fluctuations can be reduced to the study of the equation of motion for the variable $\mu_S \equiv -\sqrt{2\kappa}a[\delta\varphi + (\varphi_0'/\mathcal{H})\Phi]$, where $\kappa \equiv 8\pi G$. Its equation of motion is very similar to that of the gravitational waves [18,19]:

$$\mu_S'' + \left[k^2 - \frac{(a\sqrt{\gamma})''}{(a\sqrt{\gamma})} \right] \mu_S = 0. \quad (3)$$

The integration of (2) and (3) leads to the primordial spectrum of the fluctuations. For the initial conditions we assume that the scalar and tensor perturbations are in the quantum vacuum state when the scale of interest was well within the Hubble radius ($1/k_{\text{ph}} \ll c/H$) during the early stages of inflation. Therefore all fluctuation

variables are quantum operators during inflation. After inflation, the Universe is filled with baryons, photons, neutrinos and (cold) dark matter. For that epoch, the perturbed Einstein equations cannot be reduced to the simple form of Eqs. (2) and (3) and need to be integrated numerically. This leads to the transfer functions.

The cosmological perturbations induce anisotropies in the temperature of the CMBR, which have been detected by COBE [21] first. This is the Sachs-Wolfe effect [22]. Since it does not depend on the photon frequency, the black body shape of the photon spectrum is conserved from the last scattering surface to its observation today [23]. The measured anisotropies in the photon intensity translate into anisotropies in the temperature of the black body.

For the temperature fluctuations we introduce the abbreviation $\Delta(\vec{e}) \equiv (\delta T/T)(\vec{e})$, where \vec{e} characterizes the direction of the beam on the celestial sphere. The contributions of the scalar and tensor perturbations are given by:

$$\Delta^S(\vec{e}) = \frac{1}{4}\delta_\gamma + \Phi - e^i \partial_i v + \int_{\eta_{\text{lss}}}^{\eta_0} d\bar{\eta} \frac{\partial}{\partial \eta} (\Phi + \Psi) , \quad (4)$$

$$\Delta^T(\vec{e}) = -\frac{1}{2}e^i e^j \int_{\eta_{\text{lss}}}^{\eta_0} d\bar{\eta} \frac{\partial}{\partial \eta} h_{ij} . \quad (5)$$

The first three terms of the scalar contribution are evaluated on the last scattering surface, i.e. at η_{lss} . They represent the intrinsic fluctuations, the Sachs-Wolfe effect and the Doppler effect. The forth term is the so-called integrated Sachs-Wolfe effect. The integration is performed along the photon trajectory, which is parameterized by the conformal time here. η_0 denotes the conformal time at observation today. δ_γ is the perturbed density contrast of the photons and v the perturbed velocity of the photon fluid. For large angular scales only the first two terms are important. For isentropic (sometimes called adiabatic) perturbations the scalar part reduces to:

$$\Delta^S(\vec{e}) = \frac{1}{3}\Phi(\vec{e}) + (\dots) . \quad (6)$$

Usually, the CMBR anisotropies are expressed through the multipole moments C_l . The C_l are the coefficients in an expansion over Legendre polynomials of the CMBR temperature two-point correlation:

$$\langle \Delta^{S,T}(\vec{e}_1) \Delta^{S,T}(\vec{e}_2) \rangle = \frac{1}{4\pi} \sum_l (2l+1) C_l^{S,T} P_l(\cos \delta) , \quad (7)$$

where $\cos \delta \equiv \vec{e}_1 \cdot \vec{e}_2$. The brackets $\langle \rangle$ denote the averaging over many ensembles. Averages over many ensemble cannot be replaced by spatial averages on the celestial sphere due to the lack of ergodicity of the stochastic process $\Delta(\vec{e})$, see Ref. [24]. If, nevertheless, we do this the error made can be quantified by mean of the cosmic variance.

The computation of the multipoles for a given model requires the knowledge of the initial spectrum of the fluctuations and of the transfer function. The power spectrum of the Bardeen potential is defined in terms of the two-point correlator for the operator $\hat{\Phi}(\eta, \mathbf{x})$:

$$\langle 0 | \hat{\Phi}(\eta, \mathbf{x}) \hat{\Phi}(\eta, \mathbf{x} + \mathbf{r}) | 0 \rangle \equiv \int_0^\infty \frac{dk}{k} \frac{\sin kr}{kr} k^3 P_\Phi(\eta, k) . \quad (8)$$

Similarly, the power spectrum of gravitational waves is defined as:

$$\langle 0 | \hat{h}_{ij}(\eta, \mathbf{x}) \hat{h}^{ij}(\eta, \mathbf{x} + \mathbf{r}) | 0 \rangle \equiv \int_0^\infty \frac{dk}{k} \frac{\sin kr}{kr} k^3 P_h(\eta, k) . \quad (9)$$

A priori, the primordial power spectra are time dependent quantities. However, for the multipoles between $l = 2$ and $l = 2000$, we are interested in scales which are well beyond the horizon at the end of inflation. For those scales the power spectra do not evolve in time during inflation and they can be written as:

$$k^3 P_\Phi(k) = A_S^i \left(\frac{k}{k_0} \right)^{n_S-1} , \quad k^3 P_h(k) = A_T^i \left(\frac{k}{k_0} \right)^{n_T} , \quad (10)$$

where the spectral indexes n_S , n_T and the amplitudes A_S^i , A_T^i are independent quantities and k_0 is an arbitrarily fixed scale. The spectral indexes can also be determined from $n_S - 1 \equiv d \ln(k^3 P_\Phi) / d \ln k$ and $n_T \equiv d \ln(k^3 P_h) / d \ln k$.

An accurate calculation of the multipole moments requires numerical computations. However, for small l , the approximate equation (6) can be used. For density perturbations [25] this leads to:

$$C_l^S = \frac{4\pi}{9} \int_0^\infty \frac{dk}{k} j_l^2(kr_{\text{lss}}) T_\Phi(kr_{\text{lss}} \rightarrow 0) \times A_S^i \left(\frac{k}{k_0} \right)^{n_S-1} , \quad (11)$$

where j_l is the spherical Bessel function of order l and $r_{\text{lss}}^{\text{ph}} \equiv a(\eta_0)r_{\text{lss}} = a_0(\eta_0 - \eta_{\text{lss}}) \approx a_0\eta_0$ is the comoving line-of-sight distance to the last scattering surface. We adopt the convenient convention $k_0 = 1/r_{\text{lss}}$ throughout the rest of this work.

$T_\Phi(kr_{\text{lss}} \rightarrow 0)$ is the transfer function for superhorizon modes. It is approximatively k independent and therefore only the amplitude is modified but not the spectral index. The domain of validity of the latter approximation can be evaluated as follows. In the integral (11) the main contribution comes from the modes around $kr_{\text{lss}} \sim l+1$. We use that to estimate for which multipole moments the k independent transfer function is good enough. The mode whose wavelength is equal to the Hubble radius today, i.e. such that $2\pi a_0/k = l_H(\eta_0)$, has $k\eta_0 = 4\pi$.

Therefore the constant superhorizon transfer function is a reasonably good approximation if $(l+1)/r_{\text{lss}} \ll 4\pi/\eta_0$, that is to say $l \ll 10$. This is a very optimistic estimate since it does not take into account the first approximation, made in Eq. (6), on which the validity of Eq. (11) rests. We will come back to this question in the last section of this article.

With the above approximations the quadrupole can be calculated exactly [25]. The result reads:

$$C_2^S = \frac{\pi^2}{9} 2^{n_S-2} \frac{\Gamma[3-n_S]\Gamma[2+(n_S-1)/2]}{\Gamma^2[(4-n_S)/2]\Gamma[4-(n_S-1)/2]} A_S, \quad (12)$$

where $A_S \equiv A_S^i T_\Phi(kr_{\text{lss}} \rightarrow 0)$.

For gravitational waves we obtain the following expression [26]:

$$C_l^T = \frac{9\pi}{4} (l-1)l(l+1)(l+2) \times \int_0^\infty \frac{dk}{k} |I_l(kr_{\text{lss}})|^2 A_T \left(\frac{k}{k_0}\right)^{n_T}, \quad (13)$$

where the function $I_l(y)$ is defined by:

$$I_l(y) \equiv \int_0^y \frac{j_2(x)j_l(y-x)}{x(y-x)^2} dx. \quad (14)$$

The superhorizon transfer function for gravitational waves does not appear explicitly because it is equal to one. As a consequence we can write $A_T^i \equiv A_T$. The computation of C_l^T is more complicated than the calculation of C_2^S . The integral I_2 can be calculated exactly in terms of special functions, see Ref. [26]. However, the second integration over k cannot be performed analytically and we must rely on numerical integration.

Below we will be interested in the ratio of tensor to scalar quadrupole contributions [27–30]:

$$R \equiv \frac{C_2^T}{C_2^S}. \quad (15)$$

Expressed in terms of the tensor spectral index this is the so-called consistency equation of inflation.

We have seen that the calculation of C_l requires the knowledge of the transfer function and of the primordial spectrum. In principle, $T_\Phi(kr_{\text{lss}})$ is known accurately as the result of numerical calculations, e.g. see Refs. [31]. When we calculate the quadrupoles using Eqs. (11) or (13) we make three approximations: the slow-roll approximation (see below), a long wavelength approximation for the transfer function, and we neglect the contribution of radiation (pure matter assumption) to the expansion of the Universe at the photon decoupling. The long wavelength approximation results in neglecting other contributions besides (6) in the Sachs-Wolfe effect for scalars and in considering that the tensor and scalar superhorizon transfer functions are constant. The pure matter assumption results in a small error in the numerical value of

$T_\Phi(kr_{\text{lss}} \rightarrow 0)$. However, for small values of l , we expect that the errors are mainly due to slow-roll.

In order to test this claim quantitatively and to quantify the contribution to the total error coming from the transfer function, we compute the scalar multipole moments for low l numerically with CMBFAST [32] for the following values of the cosmological parameters: $H_0 = 50 \text{ km/s/Mpc}$, $\Omega_0 = 1$, $\Omega_{\text{CDM}} = 0.95$, $\Omega_B = 0.05$. We compare them to the multipole moments given by Eq. (11) with a constant transfer function. The code CMBFAST automatically normalizes to the COBE result [21]. The result is expressed by the band powers $(\delta T_l/T_0)^2 \equiv l(l+1)C_l/(2\pi)$, where $T_0 \approx 2.73 \text{ K}$ is the average temperature of the CMBR. For a flat ($n_S = 1$) primordial spectrum, CMBFAST gives $\delta T_2 \approx 27.5 \mu\text{K}$ or $Q_{\text{rms-PS}} \approx 17.8 \mu\text{K}$, where the quadrupole rms fluctuation is given by $Q_{\text{rms-PS}} \equiv T_0 \sqrt{(5/4\pi)C_2}$. We normalize the amplitude A_S in Eq. (11) to the latter value of the quadrupole. In Fig. (1) we plot the differences of both calculations, divided by the CMBFAST results, and express this number as the error in %. The error in the quadrupole (12) vanishes “by construction”. Equation (11) shows that $\delta T_l = T_0 \sqrt{A_S}/3 = Q_{\text{rms-PS}} \sqrt{12/5}$, whereas the CMBFAST- δT_l is l -dependent, despite both band powers are calculated from the same primordial spectrum. The difference between both band powers is exclusively due to the use of different transfer functions and to the neglection of the Doppler and integrated Sachs-Wolfe effects. In this way, we can isolate and estimate the error coming from the long wavelength approximation, being given that the spectrum is normalized to COBE.

A similar study has been done in Ref. [33]. The errors given in that article differ from those obtained here because a different normalization is used. In Ref. [33], the spectrum is normalized to the multipole moment C_{10} instead of the quadrupole. As a consequence, the error in C_{10} also vanishes “by construction”. This shows that this way of estimating the error coming from the long wavelength approximation is not independent of the normalization chosen for the spectrum.

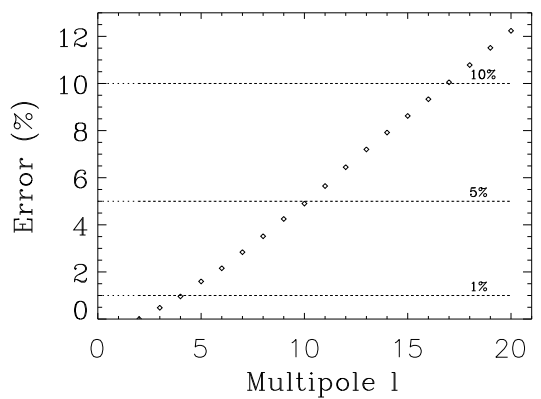


FIG. 1. Error due to the long wavelength approximation in the transfer function for the scalar multipoles with a flat primordial spectrum. The exact multipoles are calculated by means of the CMBFAST code.

This plot confirms the importance of the transfer function and the analytical estimates made at the beginning of this article. The error is below 1% only for $l < 4$. For C_{10} , which is often used to normalize the spectrum, the effect of the subleading terms in k is already 5%. Since we would like to test the slow-roll error at 1% level, we restrict ourselves to the study of the errors for the quadrupoles. The error from the pure matter assumption has not been fully accounted for by this method, because we do not test the error in the numerical value of $T_\Phi(kr_{\text{lss}} \rightarrow 0)$ when we normalize the quadrupole to the COBE result. Since this error is a pure overall numerical factor, it does not affect our conclusions. Thus for our purpose the error coming from the transfer function can be ignored for the quadrupole moments and a few higher moments.

III. PREDICTIONS OF POWER-LAW INFLATION

In this section, we turn to the study of power-law inflation. This model is of particular importance because it allows to calculate all quantities of interest exactly. Moreover, this exact result is at the basis of the slow-roll approximation.

Power-law inflation is given by the following solution for the scale factor and the scalar field:

$$a(\eta) = l_0 |\eta|^{1+\beta}, \quad \varphi = \varphi_i + \frac{m_{\text{Pl}}}{2} \sqrt{\frac{\gamma}{\pi}} (1 + \beta) \ln |\eta|, \quad (16)$$

where m_{Pl} is the Planck mass and φ_i is the initial value of the scalar field at conformal time η_i . In this model inflation occurs if $\beta < -2$ (we do not consider the case where $-2 < \beta < -1$ which cannot be realized with a single scalar field). The quantity l_0 has the dimension of a length and its value will roughly determine the amplitude of the CMBR fluctuations today. In the particular case of power-law inflation, the function $\gamma(\eta)$ is a constant equal to $(2+\beta)/(1+\beta)$. For $-\infty < \beta < -2$, γ goes from one to zero, this last value corresponding to the de Sitter spacetime. The scale factor and scalar field of Eqs. (16) are solutions of the Einstein equations for the scalar field potential:

$$V(\varphi) = V_i \exp \left[\frac{4\sqrt{\pi}}{m_{\text{Pl}}} \sqrt{\gamma} (\varphi - \varphi_i) \right], \quad (17)$$

where V_i is the value of the potential at η_i .

A. Density perturbations

The effective potential for density perturbations, $U_S \equiv (a\sqrt{\gamma})''/(a\sqrt{\gamma})$, see Eq. (3), reads:

$$U_S(\eta) = \frac{(\beta+1)\beta}{\eta^2}. \quad (18)$$

This simple form of the potential allows an exact integration of Eq. (3). The solution is expressed in terms of Bessel functions. This provides the initial power spectrum, i.e. A_S^i and n_S . In order to evolve the superhorizon spectrum, we can rely on the conservation law [34,20] for the quantity: $\xi \equiv (\mathcal{H}^{-1}\Phi' + \Phi)/\gamma + \Phi$. This gives the superhorizon transfer function: $T_\Phi(k \rightarrow 0) = [2(2\beta+3)^2]/[25\gamma^2(1+\beta)^2]$. Then the amplitude of the scalar quadrupole and the spectral index take the form:

$$A_S = \frac{l_{\text{Pl}}^2}{l_0^2} \frac{9}{25\pi\gamma} f(\beta), \quad n_S = 2\beta + 5 = \frac{1-3\gamma}{1-\gamma}, \quad (19)$$

where

$$f(\beta) \equiv \frac{1}{\pi} \left[\frac{\Gamma(-\beta - 1/2)}{2^{\beta+1}} \right]^2, \quad (20)$$

which is unity for $\beta = -2$. As expected, the amplitude of scalar perturbations is roughly determined by the ratio l_{Pl}/l_0 . Very often the final spectrum is expressed in terms of the Hubble rate at some time η_* , instead of the scale l_0 . We have $H_* \equiv H(\eta_*) = -[(1+\beta)/l_0]|\eta_*|^{-2-\beta}$ and therefore the amplitude now reads:

$$A_S = l_{\text{Pl}}^2 H_*^2 \frac{9}{25\pi\gamma} f(\beta) |1 + \beta|^{2(\beta+1)}. \quad (21)$$

The amplitude A_S is displayed as a function of γ in Fig. III B. It diverges in the de Sitter limit $\gamma \rightarrow 0$.

B. Gravitational waves

The calculation of the spectrum for gravitational waves is performed along the same lines as above. The effective potential is the same as for density perturbations, i.e. $U_T \equiv a''/a = \beta(1+\beta)/\eta^2$. Since the superhorizon transfer function is equal to one, A_T and n_T can be written as:

$$A_T = \frac{l_{\text{Pl}}^2}{l_0^2} \frac{16}{\pi} f(\beta), \quad n_T = 2\beta + 4 = -\frac{2\gamma}{1-\gamma}. \quad (22)$$

For power-law inflation, the relation $n_S = n_T + 1$ holds. In terms of H_* the amplitude is given by

$$A_T = l_{\text{Pl}}^2 H_*^2 \frac{16}{\pi} f(\beta) |1 + \beta|^{2(\beta+1)}. \quad (23)$$

Figure III B shows the scalar and tensor amplitudes (21) and (23), respectively. For $\gamma > 9/400 = 0.0225$ the tensor mode dominates.

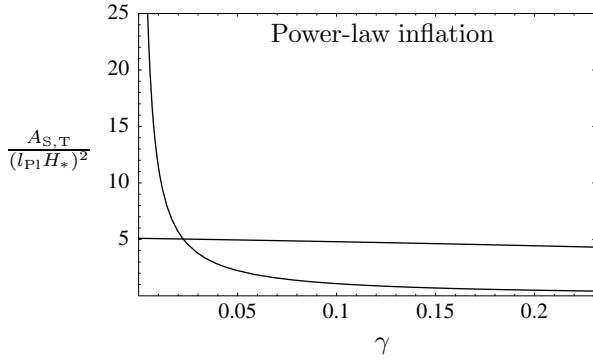


FIG. 2. The amplitudes of scalar and tensor perturbations. In the de Sitter limit $\gamma \rightarrow 0$ the scalar amplitude diverges. For larger values of γ the perturbations are dominated by the tensor mode. The plot range of γ corresponds to the allowed values for n_S from the two sigma COBE error, i.e. n_S goes from 0.6 to 1 for power-law inflation.

Using Eqs. (11) and (13), the quadrupoles can easily be computed. They are displayed in Fig. 3.

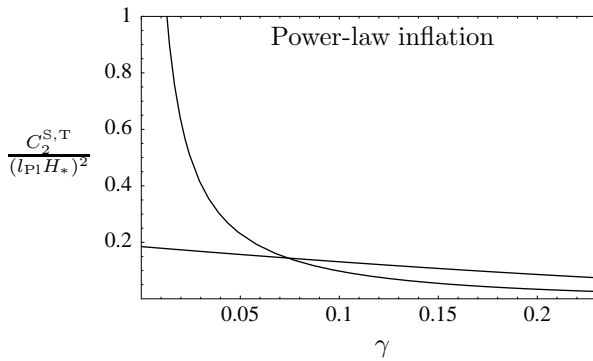


FIG. 3. The quadrupole moments of scalar and tensor perturbations.

The plot range of γ corresponds to the allowed values for n_S from COBE ($n_S = 1.2 \pm 0.3$ [21]) in a 2σ interval, i.e. for n_S between 0.6 and 1 for power-law inflation. Compared to the amplitudes the importance of the tensor mode is slightly suppressed, it becomes the dominant mode at $\gamma \gtrsim 0.07$.

C. T/S in power-law inflation

We calculate the ratio R for power-law inflation:

$$R = 13.86\gamma F[n_T(\gamma)] = -6.93 \frac{n_T}{1 - \frac{n_T}{2}} F(n_T), \quad (24)$$

where the function $F(n_T)$ is given by:

$$F(n_T) \equiv 496.1 \times 2^{1-n_T} \frac{\Gamma^2(\frac{3-n_T}{2})\Gamma(4-\frac{n_T}{2})}{\Gamma(2-n_T)\Gamma(2+\frac{n_T}{2})}$$

$$\times \int_0^\infty dk k^{n_T-1} |I_2(k)|^2. \quad (25)$$

In this expression we have used the equation $n_S = n_T + 1$, valid for power-law inflation only, to express everything in terms of n_T . We have $\int_0^\infty dk k^{-1} |I_2(k)|^2 = 2.139 \times 10^{-4}$ such that $F(n_T = 0) = 1$. R versus γ is plotted in Fig. 4. This plot demonstrates that within the two sigma error bars of COBE, there is a large parameter space where the tensor mode dominates the scalar modes, see e.g. Refs. [28,30] for a more detailed discussion.

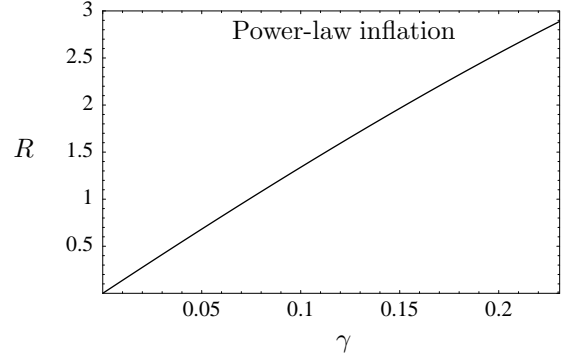


FIG. 4. The tensor to scalar ratio of the quadrupole moments.

IV. PREDICTIONS OF SLOW-ROLL INFLATION

For a general model of inflation exact solutions are not available. Generically, the potentials U_S and U_T are different but nevertheless their shape is similar. A sketch of the generic form of U_S and U_T is displayed in Fig. 5. The details of the realistic reheating transition are not taken into account in this simple figure. During the radiation dominated era the potential goes to zero, since $a \propto \eta$.

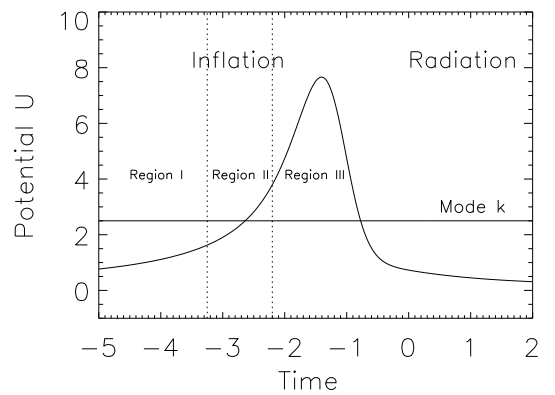


FIG. 5. Sketch of the effective potential for density perturbations and/or gravitational waves during inflation and radiation.

For a given mode k , the inflationary epoch can be divided into three stages, see Fig. 5. In region I the mode k is subhorizon. In that case the effective potential is small compared to k^2 . In the limit $k/(aH) \rightarrow \infty$ for fixed k , the vacuum fluctuations are given by, see Ref. [20]:

$$\mu_{S,T}(\eta) \rightarrow \mp 4\sqrt{\pi}l_{\text{Pl}} \frac{e^{-ik(\eta-\eta_i)}}{\sqrt{2k}} , \quad (26)$$

respectively. In region III the mode is superhorizon. In the limit $k/(aH) \rightarrow 0$ at fixed k , the potential term is dominant, and the “exact” solutions read:

$$\mu_S(\eta) = C_S(a\sqrt{\gamma})(\eta) \times \left[1 - k^2 \int^\eta \frac{1}{(a^2\gamma)(\bar{\eta})} \int^{\bar{\eta}} (a^2\gamma)(\tilde{\eta}) d\tilde{\eta} d\bar{\eta} \right] , \quad (27)$$

$$\mu_T(\eta) = C_T a(\eta) . \quad (28)$$

Usually, density perturbations are described in terms of the Bardeen potential Φ instead in terms of μ_S . The order k^2 term is necessary to obtain the leading order expression for the Bardeen potential, since $\Phi = [\mathcal{H}\gamma/(2k^2)][\mu_S/(a\sqrt{\gamma})]'$, see Refs. [20,19]. Thus, in region III, the superhorizon Bardeen potential is given by:

$$\Phi(\eta) = \frac{C_S \mathcal{H}}{2a^2} \int^\eta a^2\gamma d\bar{\eta} . \quad (29)$$

Our aim is to calculate the spectra at the end of inflation, i.e. in region III. The time dependence of the solutions in this region is known and the difficulty lies in the calculation of the constants C_S and C_T . Since the solutions are uniquely determined in region I, this amounts to join the super- and subhorizon solutions. Therefore we need to know the behavior of the perturbations in region II.

A popular approach is the slow-roll approximation [9,11]. The idea is that there was an epoch during inflation where the scalar field was rolling down its potential $V(\varphi)$ very slowly. Under certain conditions (see below) this is close to the behavior during power-law inflation and the exact solutions from power-law inflation are used in region II to interpolate between the sub- and superhorizon solutions.

Slow roll is controlled by the three (leading) slow-roll parameters (see e.g. Ref. [11]) defined by:

$$\epsilon \equiv 3 \frac{\dot{\varphi}^2}{2} \left(\frac{\dot{\varphi}^2}{2} + V \right)^{-1} = - \frac{\dot{H}}{H^2} , \quad (30)$$

$$\delta \equiv - \frac{\ddot{\varphi}}{H\dot{\varphi}} = - \frac{\dot{\epsilon}}{2H\epsilon} + \epsilon , \quad (31)$$

$$\xi \equiv \frac{\dot{\epsilon} - \dot{\delta}}{H} . \quad (32)$$

We see in particular that $\gamma(\eta) = \epsilon$ in region II. The equations of motion for ϵ and δ can be written as:

$$\frac{\dot{\epsilon}}{H} = 2\epsilon(\epsilon - \delta) , \quad \frac{\dot{\delta}}{H} = 2\epsilon(\epsilon - \delta) - \xi . \quad (33)$$

The slow-roll conditions are satisfied if ϵ and δ are much smaller than one and if $\xi = \mathcal{O}(\epsilon^2, \delta^2, \epsilon\delta)$. From Eqs. (33), it is clear that this amounts to consider ϵ and δ as constants. This property is crucial for the calculation of the perturbations.

For power-law inflation the slow-roll parameters satisfy:

$$\epsilon = \delta < 1 , \quad \xi = 0 . \quad (34)$$

Therefore the slow-roll conditions are fulfilled if $\epsilon \ll 1$, that is to say if β is close to -2 (scale invariance). In fact, the slow-roll approximation is an expansion around power-law inflation with $0 < -(\beta + 2) \ll 1$. To illustrate this point, let us consider the exact equation:

$$\eta = - \frac{1}{aH} + \int da \frac{\epsilon}{a^2 H} . \quad (35)$$

If we assume that ϵ is a constant, the previous equation reduces to $aH \approx -(1 + \epsilon)/\eta$. This is equivalent to a scale factor which behaves like:

$$a(\eta) \approx l_0 \eta^{-1-\epsilon} . \quad (36)$$

Interestingly enough, the effective power index at leading order depends on ϵ only.

A. Density perturbations

The effective potential of density perturbations can be calculated in terms of the slow-roll parameters exactly. The result is:

$$U_S(\eta) = a^2 H^2 [2 - \epsilon + (\epsilon - \delta)(3 - \delta) + \xi] . \quad (37)$$

In the slow-roll approximation $a^2 H^2 \approx \eta^{-2}(1 + 2\epsilon)$ and the effective potential reduces to $U_S \approx (2 + 6\epsilon - 3\delta)\eta^{-2}$. Since ϵ and δ must be seen as constants in the slow-roll approximation, the equation of motion (3) is of the same type as in power-law inflation. The solutions are given by Bessel functions:

$$\mu_S = (k\eta)^{1/2} [B_1 J_{\nu_S^{(\text{sr})}}(k\eta) + B_2 J_{-\nu_S^{(\text{sr})}}(k\eta)] , \quad (38)$$

whose order is given by

$$\nu_S^{(\text{sr})}(\eta) = - \frac{3}{2} - 2\epsilon + \delta . \quad (39)$$

A comment is in order here: The potential U_S depends on the scale factor and its derivatives only. One could think, looking at Eq. (36), that U_S also depends on ϵ only. This is not the case. The reason is that U_S contains terms like $\dot{\epsilon}/\epsilon$ (for example) which are linear in δ , see Eqs. (33). First one must calculate all derivatives, replace them with their expression in terms of ϵ and δ , and only then consider that the slow-roll parameters are constant.

We would also like to stress that keeping higher orders in ϵ does not make sense. If terms of quadratic order in the slow-roll parameters are kept, the solution for density perturbations in region II can no longer be expressed in terms of Bessel functions. This is because the slow-roll parameters can no longer be considered as constant in time, see Eqs. (33). Therefore any considerations at this order in the framework of the slow-roll approximation is meaningless. The same conclusion has been obtained by Wang, Mukhanov, and Steinhardt [10].

Let us now calculate the constant C_S . The first step is to match the solutions of region I and II. This procedure fixes B_1 and B_2 . Using Eqs. (26) and (27), one obtains: $B_1/B_2 = -e^{i\pi\nu_S^{(\text{sr})}}$ and $B_1 = 2i\pi l_{\text{Pl}} \exp[i\nu_S^{(\text{sr})}(\pi/2) - i(\pi/4) + ik\eta_*]/(\sqrt{k} \sin \pi\nu_S^{(\text{sr})})$. Note that B_1 and B_2 do not depend on the time at which the matching between regions I and II is performed. The joining between regions II and III remains to be performed at some time η_S , which will be fixed below. Expanding everything up to next-to-leading order in the slow-roll parameters, one obtains:

$$|C_S|^2 = \frac{l_{\text{Pl}}^2}{l_0^2} \frac{8\pi}{\epsilon} \left[1 - 2(C + \ln k)(2\epsilon - \delta) + 2(\delta - \epsilon) \ln |\eta_S| \right] k^{-3}, \quad (40)$$

with $C \equiv \gamma_E + \ln 2 - 2 \approx -0.7296$, $\gamma_E \approx 0.5772$ being the Euler constant. The Bardeen potential given in Eq. (29) is now completely specified. Note that $\gamma(\eta)$ in Eq. (29) is a time dependent function, evaluated in region III, whereas ϵ in Eq. (40) is a constant parameter, which is fixed by $\epsilon = \gamma(\eta_S)$.

For scalar perturbations it is useful to evaluate the quantity

$$\zeta = -\frac{\mu_S}{2a\sqrt{\epsilon}}, \quad (41)$$

which is a *constant* for the dominant mode at superhorizon scales [34,7,20]. The quantity $-\zeta$ is denoted \mathcal{R} in Ref. [11]. Instead of expressing the spectrum in terms of the ratio l_{Pl}/l_0 , it is usual to write it in terms of the Hubble rate at some time η_* . Of course, there is nothing deep in this choice and one could have kept working with l_{Pl}/l_0 . A priori, the value of η_* is arbitrary and could either be in regions I, II or III. However, in order to make contact with the literature, we will assume that η_* is in region II. Then, in the slow-roll approximation, the value of $H(\eta_*)$ can be written as:

$$H_* \equiv H(\eta_*) = \frac{1}{l_0} [1 + \epsilon(1 + \ln |\eta_*|)]. \quad (42)$$

In Ref. [11], η_* is the time which satisfies the relation $a(\eta_*)H(\eta_*) = k$ for each mode k . In other words, we have $\eta_* = \eta_*(k)$. In this article, we adopt another convention. We choose η_* to be the time such that $a(\eta_*)H(\eta_*) = k_0$,

where k_0 is an arbitrary fixed scale, already introduced in Eqs. (10). Then, a straightforward calculation gives

$$k^3 P_\zeta(k) = \frac{l_{\text{Pl}}^2 H_*^2}{\pi\epsilon} \left\{ 1 - 2\epsilon - 2 \left[C + \ln \frac{k}{k_0} \right] (2\epsilon - \delta) + 2(\delta - \epsilon) \ln \left| \frac{\eta_S}{\eta_*} \right| \right\}. \quad (43)$$

The matching time η_S remains to be fixed by a physical argument. To our knowledge, this issue has been overlooked in the literature so far. All works on the slow-roll approximation, starting with Ref. [9], have tacitly assumed that $\eta_S/\eta_* = 1$, without further justification. A priori, an equally good choice would be, for example, when the mode k_0 crosses the effective potential, i.e. when $k_0^2 = U_S(\eta_S)$. It is easy to show that this boils down to the choice $\eta_S/\eta_* = \sqrt{2}$. It is important to realize that different choices for the ratio η_S/η_* lead to different observational predictions. Although a change in η_S would not change the spectral index, it would change the amplitude of scalar perturbations and the ratio of tensor to scalar contributions R .

The missing physical argument comes from a new family of exact solutions which has a slow-roll regime in a certain limit. One exact solution is of course power-law inflation, but it does not help for the purpose of fixing η_S/η_* , because the spectrum does not depend on η_S/η_* for $\delta = \epsilon$. These solutions are found by the ansatz

$$a\sqrt{\gamma} = \frac{A}{|\eta|^\alpha}, \quad (44)$$

where A and α are two free parameters. This defines a two-parameters family of exact solution. Note that this family is not equivalent to power-law inflation. The power-law model ($A = l_0\sqrt{\gamma(\beta)}$, $\alpha = -1 - \beta$) is a subclass of this two-parameter family. Of course, this is because $a(\eta) \propto |\eta|^\alpha$ is just a solution of Eq. (44), viewed as a second order differential equation for the scale factor, but not the general solution. The limit A to zero and α close to one gives a slow-roll inflation model. The particular case $\alpha = 1$ was already found recently by Starobinsky [15]. This one parameter family of solutions is characterized by a flat spectrum, $n_S = 1$. Eq. (44) is a generalization of Starobinsky's original ansatz [15]. The spectrum may be calculated exactly to read

$$k^3 P_\zeta(k) = \frac{l_{\text{Pl}}^2}{\pi^2 A^2} 2^{2\alpha} \Gamma^2 \left(\alpha + \frac{1}{2} \right) k^{-2(\alpha-1)}. \quad (45)$$

The case $\alpha = 1$ gives $k^3 P_\zeta(k) = l_{\text{Pl}}^2/(\pi A^2)$ and coincides with the result of Ref. [15].

We now need to calculate the slow-roll spectrum for this new class of solutions. A comparison with Eq. (43) will allow us to fix the ratio η_S/η_* . Let us first determine the slow-roll parameters. In the slow-roll approximation we find

$$\frac{(a\sqrt{\gamma})'}{a\sqrt{\gamma}} = -\frac{1}{\eta}(1 + 2\epsilon - \delta), \quad (46)$$

whereas insertion of the ansatz (44) into this equation gives $(a\sqrt{\gamma})'/(a\sqrt{\gamma}) = -\alpha/\eta$. Therefore, one has $2\epsilon = (\alpha - 1) + \delta$ and especially $2\epsilon = \delta$ if $\alpha = 1$. It is interesting to note that we no longer have the relation $\epsilon = \delta$ typical of power-law inflation. Let us also emphasize that the two-parameter family is the only family of exact solutions which permits a slow roll approximation. Eq. (46) is a necessary condition for the validity of the slow-roll approximation. This equation can be viewed as a first-order differential equation for the quantity $a\sqrt{\gamma}$. Integration of this equation leads to the ansatz given in Eq. (44). Therefore our determination of the ratio η_S/η_* is general. The value of A in the slow-roll limit is obtained from $A = a\sqrt{\gamma}|\eta|^\alpha$ and is expressed in terms of H_* with the help of (35). This gives $A^2 = \epsilon H_*^{-2}[1+2\epsilon-2(2\epsilon-\delta)\ln k_0]$. Thus we obtain the slow roll spectrum from Eq. (45):

$$k^3 P_\zeta(k) = \frac{l_{\text{Pl}}^2 H_*^2}{\pi\epsilon} \left\{ 1 - 2\epsilon - 2[C + \ln \frac{k}{k_0}](2\epsilon - \delta) \right\}. \quad (47)$$

A comparison with (43) shows that

$$\eta_S = \eta_*. \quad (48)$$

Note that we could have derived the slow-roll spectrum of ζ from the exact spectrum (45) right from the beginning, by approximating it in the slow-roll regime. However, we have chosen to take the Bessel function/horizon crossing approach, because it is this approach which has been discussed in the literature. Let us note that the transfer function for ζ is unity. This means that the spectrum of ζ during the matter dominated era is identical to the spectrum at the end of inflation (region III).

We are mostly interested in the spectrum of the metric potential Φ since this quantity appears in the calculations of the multipole moments, see Eq. (11). If we assume that the Universe is matter dominated at the surface of last scattering, then the conservation law provides us with the relation $\zeta = (5/3)\Phi$. Then, the spectrum of the Bardeen potential follows from (47) as:

$$n_S^{(\text{sr})} = 1 - 4\epsilon + 2\delta, \quad (49)$$

$$A_S^{(\text{sr})} = l_{\text{Pl}}^2 H_*^2 \frac{9}{25\pi\epsilon} [1 - 2\epsilon - 2C(2\epsilon - \delta)]. \quad (50)$$

These expressions are consistent with (4.3) and (5.1) of [11]. The amplitude of scalar perturbations blows up when the slow-roll approximation becomes accurate, i.e. when ϵ goes to zero.

To end this section, let us make a last comment. It is clear from the previous considerations that we need the slow-roll approximation in region II only. In particular, this scheme of approximation is not needed in region III since the “exact” solution is known. However, one may wish to use it in region III also. Then, in this region, the Bardeen potential is given by $\Phi \approx (C_S/2)\epsilon(1 - 3\epsilon + 2\delta)$. The long-wavelength transfer function, which allows to pass from the end of inflation to the matter dominated

epoch can be expressed as $T_\Phi \approx [9/(25\epsilon^2)](1 + 6\epsilon - 4\delta)$. Using the two previous formula, one can show that one recovers the spectrum given in Eqs. (49) and (50). However, in principle, this method is not appropriate since we use an approximated solution whereas an exact one is available.

B. Gravitational waves

For gravitational waves, the same lines of reasoning can be applied. In region II, the effective potential can be written as:

$$U_T(\eta) = a^2 H^2 (2 - \epsilon), \quad (51)$$

and gives in the slow-roll limit

$$U_T(\eta) \sim \frac{2 + 3\epsilon}{\eta^2}. \quad (52)$$

Therefore the matching of sub- and superhorizon solution is again reduced to power-law inflation. The solution of μ_T is similar to the one given in Eq. (38), where the effective index of the Bessel function is now given by:

$$\nu_T^{(\text{sr})}(\epsilon) = -\frac{3}{2} - \epsilon. \quad (53)$$

This solution can be used to find the constant C_T . Then, the power spectrum of gravitational waves reads

$$k^3 P_h(k) = \frac{l_{\text{Pl}}^2}{l_0^2} \frac{16}{\pi} \left(1 - 2C\epsilon - 2\epsilon \ln \frac{k}{k_0} \right), \quad (54)$$

from which we deduce that:

$$n_T^{(\text{sr})} = -2\epsilon, \quad (55)$$

$$A_T^{(\text{sr})} = l_{\text{Pl}}^2 H_*^2 \frac{16}{\pi} [1 - 2(C + 1)\epsilon]. \quad (56)$$

We see that there exists a crucial difference between density perturbations and gravitational waves. In the case of gravitational waves, the ambiguity related to the choice of the matching time is not present.

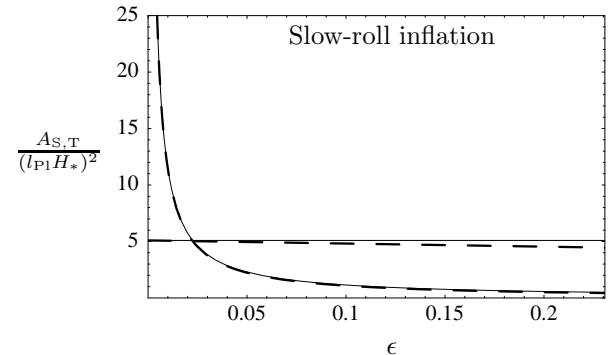


FIG. 6. The scalar and tensor amplitudes from the slow-roll approximation for $\epsilon = \delta$. The scalar amplitude diverges in the de Sitter limit $\epsilon \rightarrow 0$. The leading order is drawn by full lines, the next-to-leading order by dashed lines.

The amplitudes of scalar and tensor modes versus the slow-roll parameter ϵ are displayed in Fig. 6 for $\delta = \epsilon$ and in Fig. 7 for $\delta = 2\epsilon$ at leading and next-to-leading order. The first case is an approximation to the exact power-law result, the case $\delta = 2\epsilon$ is the slow-roll approximation to Starobinsky's exact solution.

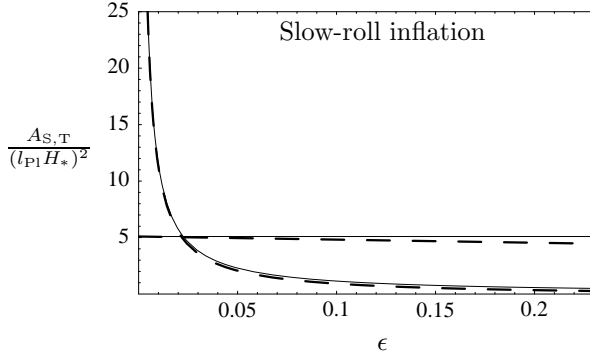


FIG. 7. The same as Fig. 6, but for $\delta = 2\epsilon$.

C. T/S in slow-roll inflation

We can now use the results of the previous sections to calculate R in the slow-roll regime at the leading and next-to-leading order. Let us first start with the calculation of C_2^S . Using Eqs. (50), (12), we find that:

$$C_2^S = l_{Pl}^2 H_*^2 \frac{\pi}{25\epsilon} g_S(n_S) [1 - 2C(2\epsilon - \delta) - 2\epsilon] , \quad (57)$$

with,

$$g_S(n_S) \equiv 2^{n_S-2} \frac{\Gamma(3-n_S)\Gamma(2+(n_S-1)/2)}{\Gamma^2[(4-n_S)/2]\Gamma[4-(n_S-1)/2]} . \quad (58)$$

Our aim is to compute C_2^S at the next-to-leading order in the slow-roll parameters. Since n_S is itself a linear function of ϵ and δ , we must expand the function $g^S(n_S)$ to the first order around $n_S = 1$. We obtain:

$$g_S(n_S) = g_S(n_S = 1) + (n_S - 1) \frac{dg_S}{dn_S}(n_S = 1) \quad (59)$$

$$= \frac{1}{3\pi} [1 + (n_S - 1)D] , \quad (60)$$

where $D \equiv \ln 2 - \Psi(2)/2 + \Psi(3/2) + \Psi(4)/2 \approx 1.1463$, with $\Psi \equiv d \ln \Gamma(x)/dx$. Expressing n_S in terms of ϵ and δ , see Eq. (49), we find the scalar quadrupole at next-to-leading order as

$$C_2^S = \frac{l_{Pl}^2 H_*^2}{75\epsilon} \left[1 - 2\epsilon - 2(D + C)(2\epsilon - \delta) \right] , \quad (61)$$

where $D + C \approx 0.4167$.

Let us now compute C_2^T . Using Eqs. (13) and (56), we find at next-to-leading order in n_T :

$$C_2^T = 0.1848 l_{Pl}^2 H_*^2 [1 - 2(B + C + 1)\epsilon] , \quad (62)$$

where the number B is defined by: $B \equiv \int_0^\infty dk k^{-1} \ln(k) I_2^2(k) / \int_0^\infty dk k^{-1} I_2^2(k) \approx 1.2878$ so that $B + C \approx 0.5582$. In Figs. 8 the scalar and tensor quadrupoles at leading and next-to-leading orders are displayed for the case $\epsilon = \delta$.

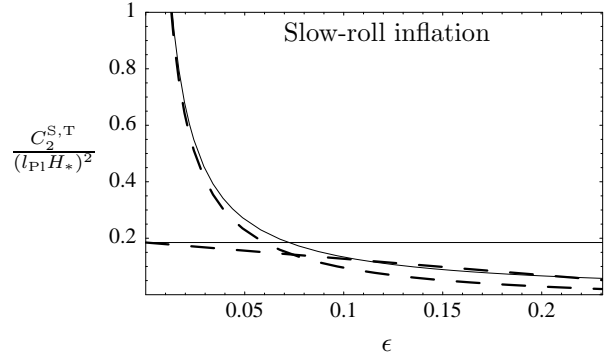


FIG. 8. The scalar and tensor quadrupole moments from the slow-roll approximation for $\epsilon = \delta$. The leading order is drawn by full lines, the next-to-leading order by dashed lines.

Taking into account the expressions for C_2^S and C_2^T given previously, we finally find the following expression for R in the slow-roll regime:

$$R = 13.86\epsilon [1 + 0.5504\epsilon - 0.8334\delta] . \quad (63)$$

At leading order we recover the so-called *consistency condition for slow-roll inflation* [11], which reads

$$R = -6.93n_T . \quad (64)$$

This equation cannot be generalized by the use of (63) to a next-to-leading order equation, because it would involve the knowledge of the order $\mathcal{O}(\epsilon^2)$ terms in n_T . As discussed above, terms of that order are not meaningful in the slow-roll approximation.

In Fig. 9, the ratio R is displayed at leading and next-to-leading order for the two cases $\epsilon = \delta$ and $2\epsilon = \delta$.

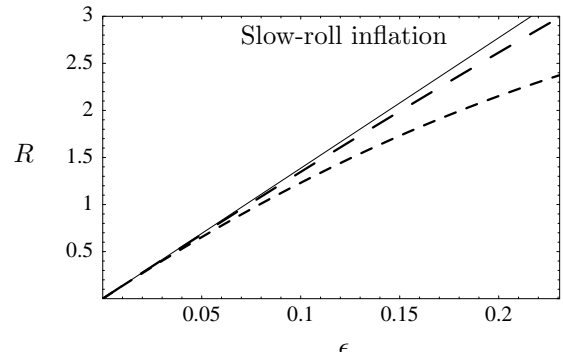


FIG. 9. The tensor to scalar ratio at leading order (full line) and at next-to-leading order for $\delta = \epsilon$ (long dashed line) and $\delta = 2\epsilon$ (short dashed line). The leading order is independent of δ .

V. DISCUSSION OF THE ERROR

The aim of this section is to quantify the magnitude of the error introduced by the slow-roll approximation. For this purpose, we compare the slow-roll predictions with the exact results of power-law inflation. We test the following quantities: $Q \in \{n_S - 1, n_T, A_S, A_T, C_2^S, C_2^T, R\}$, i.e. quantities related to the power spectra and the quadrupole moments.

We denote by Q the exact result of power-law inflation and by $Q^{(0)}$, $Q^{(1)}$ the slow-roll results at leading and next-to-leading orders, respectively. The error is estimated by calculating:

$$e_Q^{(i)} \equiv \left| \frac{Q^{(i)} - Q}{Q} \right| \times 100\%. \quad (65)$$

Let us start with an estimate of the errors in the prediction of the spectral indices n_S and n_T . For the leading order slow-roll approximation $n_T = n_S - 1 = 0$ and thus the error is $e_{n_S-1}^{(0)} = e_{n_T}^{(0)} = 100\%$, except for de Sitter inflation. It is absolutely compulsory to use the next-to-leading order result for the spectral indices. We express the error as a function of γ . The best slow-roll approximation to a power-law model is given by $\epsilon = \delta = \gamma$, and therefore $n_T^{(\text{sr})} = n_S^{(\text{sr})} - 1$ for this case. Thus from Eqs. (22) and (55) the error of the tensor spectral index from the slow-roll approximation is

$$e_{n_S-1}^{(1)} = e_{n_T}^{(1)} = \gamma \times 100\%. \quad (66)$$

Thus the next-to-leading order slow-roll approximation predicts the spectral indices with an error less than 1%, if $\gamma < 0.01$ or $0.98 < n_S < 1$.

The errors of the amplitudes and quadrupoles for the case of power-law inflation, $\epsilon = \delta$, are displayed in Figs. 10 and 11.

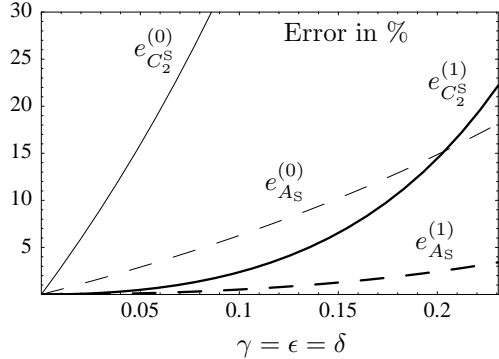


FIG. 10. The error for the scalar quantities. The full lines are the quadrupole moments, the dashed lines are the amplitudes. The thin lines are the leading order corrections, the thick lines are the next-to-leading order corrections.

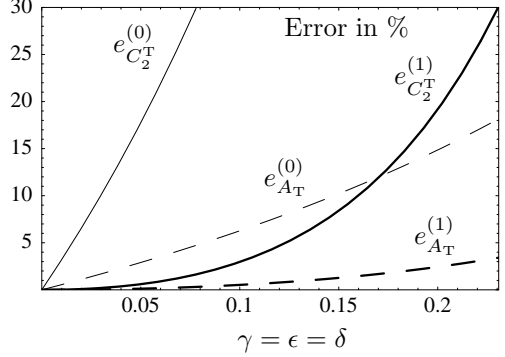


FIG. 11. The same as Fig. 10, but for the tensor amplitude and quadrupole moment. For the amplitude the error is the same as for the scalar sector, because $\epsilon = \delta$.

From these two plots, we can draw three important conclusions. Firstly, the error of the quadrupoles is larger than the error for the amplitudes. This confirms the results already obtained in Ref. [35]. This is probably true for higher multipoles as well. Secondly, in order to obtain predictions at the 1% level, the next-to-leading order is necessary. Forthcoming high precision missions, especially the MAP and PLANCK satellites, will determine the temperature correlations with a precision of a few percent. Therefore predictions from inflationary models should be made on the few percent level as well. The previous study demonstrates that the next-to-leading order of the slow-roll approximation is needed to reach this goal. Thirdly, the next-to-leading order is accurate enough if $\gamma < 0.07$ which corresponds to $0.85 < n_S$. Since the slow-roll approximation is more accurate for power-law model, it is reasonable to expect a larger error for more realistic models.

The error of the T/S ratio is displayed in Fig. 12:

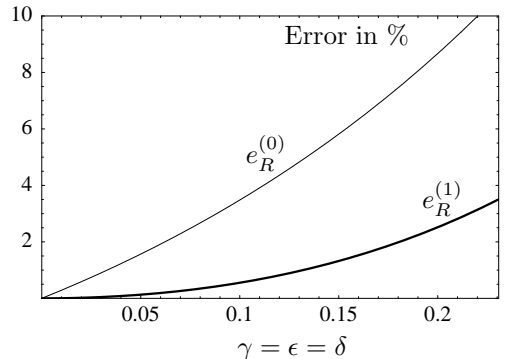


FIG. 12. The error of the tensor to scalar ratio in leading (thin line) and next-to-leading order (thick line).

We see that the error of R is less important than for the amplitudes and/or the quadrupoles. Therefore this suggests to use R to test the single scalar field/slow-roll paradigm. However, it is clear that any violation of the consistency check by the forthcoming data should be in-

terpreted as a failure of this paradigm but not as the failure of inflation itself.

We conclude that for a general model of inflation only numerical mode-by-mode integration can presently provide predictions for the CMBR with less than 1% error. This conclusion renders difficult all attempts to reconstruct the inflationary potential without the assumption of a specific slow-roll model. The reason for this is that reconstruction usually assumes that the primordial spectrum, instead of the multipoles, is measured to a high precision. We have shown in this work, that the errors in the prediction of the multipoles are easily an order of magnitude larger. A first attempt to go directly from inflation to the calculation of the multipole moments has been put forward by Grivell and Liddle [36] recently. In our opinion a purely numerical approach to this fundamental issue is not fully satisfactory — better analytic methods are needed.

ACKNOWLEDGMENTS

We would like to thank A. R. Liddle, V. F. Mukhanov, and V. Shani for valuable discussions and/or comments. D. S. thanks the Austrian Academy of Sciences for financial support. J. M. thanks Robert Brandenberger and the High Energy Group of Brown University (Providence, USA) for warm hospitality.

- [10] L. Wang, V. F. Mukhanov and P. J. Steinhardt, Phys. Lett. B **414**, 18 (1997).
- [11] J. E. Lidsey et al., Rev. Mod. Phys. **69**, 373 (1997).
- [12] E. J. Copeland et al., Phys. Rev. D **49**, 1840 (1994).
- [13] E. W. Kolb and S. L. Vadas, Phys. Rev. D **50**, 2479 (1994).
- [14] E. J. Copeland et al., Phys. Rev. D **58**, 043002 (1998).
- [15] A. A. Starobinsky, talk at DARC, Meudon, December 11, 1998, to be published in JETP Lett. **70** (1999).
- [16] J. A. Bardeen, Phys. Rev. D **22**, 1882 (1980).
- [17] L. P. Grishchuk, Zh. Eksp. Teor. Fiz. **64**, 825 (1974) [Sov. Phys. JETP **40**, 409 (1974)].
- [18] V. F. Mukhanov, Zh. Eksp. Teor. Fiz. **94**, 1 (1988) [Sov. Phys. JETP **68**, 1297 (1988)].
- [19] L. P. Grishchuk, Phys. Rev. D **50**, 7154 (1994).
- [20] J. Martin and D. J. Schwarz, Phys. Rev. D **57**, 3302 (1998).
- [21] G. Smoot et al., Astrophys. J. **396**, L1 (1992); C. L. Bennett et al., Astrophys. J. **464**, L1 (1996); K. M. Gorski et al., Astrophys. J. **464**, L11 (1996).
- [22] R. K. Sachs and A. M. Wolfe, Astrophys. J. **147**, 73 (1967).
- [23] D. J. Fixsen et al., Astrophys. J. **473**, 576 (1996).
- [24] L. P. Grishchuk and J. Martin, Phys. Rev. D **56**, 1924 (1997).
- [25] P. J. E. Peebles, Ap. J. **263**, L1 (1982). J. R. Bond and G. Efstathiou, Ap. J. **285**, L45 (1984).
- [26] A. A. Starobinsky, Sov. Astron. Lett. **11**, 133 (1985).
- [27] R. L. Davis et al., Phys. Rev. Lett. **69**, 1856 (1992). D. S. Salopek, Phys. Rev. Lett. **69**, 3602 (1992). A. R. Liddle and D. H. Lyth, Phys. Lett. B **291**, 391 (1992).
- [28] T. Souradeep and V. Sahni, Mod. Phys. Lett. **7**, 3541 (1992).
- [29] R. Crittenden et al., Phys. Rev. Lett. **71**, 324 (1993).
- [30] P. J. Steinhardt, Int. J. Mod. Phys. A **10**, 1091 (1995).
- [31] J. Bardeen et al., Astrophys. J. **304**, 15 (1986).
- [32] U. Seljak and M. Zaldarriaga, Astrophys. J. **469**, 437 (1996); CMBFAST Website: <http://www.sns.ias.edu/~matiasz/CMBFAST/cmbfast.html>.
- [33] E. Bunn and M. White, Astrophys. J. **480**, 6 (1997).
- [34] D. H. Lyth, Phys. Rev. D **31**, 1792 (1985).
- [35] D. J. Schwarz and J. Martin, astro-ph/9805313 published in: *Current Topics in Mathematical Cosmology*, Eds. M. Rainer and H.-J. Schmid (World Scientific PC, Singapore, 1998) pp. 65.
- [36] I. J. Grivell and A. R. Liddle, astro-ph/9906327 (1999).